

Horizontal bridges in polar dielectric liquids

J. Woisetschläger, A. D. Wexler, G. Holler, M. Eisenhut, K. Gatterer, E. C. Fuchs

Jakob Woisetschläger

*Experimental Turbomachinery Research and Optical Measurement Group,
Institute for Thermal Turbomachinery and Machine Dynamics, Graz University of
Technology*

Inffeldgasse 25 A, 8010 Graz, Austria

Phone: +43 316 873 7277

Fax: +43 316 873 7239

e-mail: jakob.woisetschlaeger@tugraz.at

Adam D. Wexler

*Wetsus - Center of Excellence for Sustainable Water Technology
Agora 1, 8900 CC Leeuwarden, The Netherlands*

Phone.: +31 58 284 31 89

Fax.: +31 58 284 30 01

e-mail: adam.wexler@wetsus.nl

Gert Holler

*Institute of Electrical Measurement and Measurement Signal Processing, Graz
University of Technology*

Kopernikusgasse 24/IV, 8010 Graz, Austria

Phone: +43 316 873 7269

Fax: +43 316 873 7266

e-mail: gert.holler@tugraz.at

Mathias Eisenhut

*Institute of Analytical Chemistry and Food Chemistry, Graz University of
Technology,*

Stremayrgasse 9, 8010 Graz, Austria

Karl Gatterer

*Institute of Physical and Theoretical Chemistry, Graz University of Technology
Stremayrgasse 9, 8010 Graz, Austria*

Phone: +43 316 873 32250

e-mail: gatterer@tugraz.at

Elmar C. Fuchs

Wetsus - Center of Excellence for Sustainable Water Technology

Agora 1, 8900 CC Leeuwarden, The Netherlands

Phone.: +31 58 28 43162

Fax.: +31 58 28 43001

e-mail: elmar.fuchs@wetsus.nl

Abstract: When a high-voltage direct-current is applied to two beakers filled with polar liquid dielectrics like water or methanol, a horizontal bridge forms between the two beakers. By repeating a version of Pellat's experiment it is shown that a horizontal bridge is stable by the action of electrohydrodynamic pressure. Thus the static and dynamic properties of the phenomenon called a 'floating water bridge' can be explained by the gradient of Maxwell pressure, replenishing the liquid within the bridge against any drainage mechanism. It is also shown that a number of liquids can form stable and long horizontal bridges. The stability of such a connection, and the asymmetry in mass flow through such bridges caused by the formation of ion clouds in the vicinity of the electrodes, is also discussed by two further experiments.

Keywords: optical measurement, high voltage, dielectric fluid

Introduction

In 1893 Sir William George Armstrong first reported on the formation of a horizontal bridge of water forming between two beakers filled with deionised water when a direct-current (DC) high-voltage is applied (Armstrong 1893). Recently, a number of publications made the modern scientific community aware of this experiment (Fuchs et al. 2007, 2008).

When filling glass beakers with deionised water and applying a DC voltage between 10 kV and 20 kV, a watery connection forms between the beakers. Since the experiment is stable, easy to reproduce, and grants free experimental access to water inside the bridge under variable high voltage and atmospheric conditions in air, it promises insights into basic features of dipole-dipole interaction in water (Fuchs 2010). Therefore a number of experiments in the horizontal bridge of water were performed, using neutron scattering (Fuchs et al. 2009, Fuchs et al. 2010b), visualization and optical measurement techniques (Woissetschläger et al. 2010), Raman scattering (Ponterio et al. 2010), Brillouin scattering (Fuchs et al. 2011b), zero gravity experiments (Fuchs et al. 2011a), and was discussed in relation to molecular vibration coupling (Del Giudice et al. 2010) and the influence of some electrolytes (Nishiumi and Honda 2009) and non-ionic solvents (Eisenhut et al. 2011) on the water bridge.

Due to its unique properties several authors discussed the electrohydrodynamics of such a stable and horizontal bridge of water forming between two beakers under ambient conditions in air. Widom et al. (2009) and Saija et al. (2010) stated that the high dielectric permittivity of water is the reason for a stable bridge forming and used the electrohydrodynamic Maxwell stress tensor to calculate tensions in the water bridge. A similar approach was used by Marin and Lohse (2010) to explain the stability of the horizontal bridge. While Fuchs (2010) already demonstrated that a horizontal bridge also forms in Methanol, the works of Marin and Lohse (2010) or Saija et al. (2010) discovered other polar liquids do also form horizontal bridges, e.g. Glycerol. Ponterio et al. (2010) used alternating-current (AC) experiment to form a stable water bridge, a technique used in electrohydrodynamics (EHD) whenever the screening effects of free charges want to be reduced or nullified. Finally Aerov (2010) pointed out that

a stable equilibrium for the bridge's surface is reached when the axial electric field is strong enough to counteract distortions caused by surface tension.

It must be mentioned that all EHD discussions of the horizontal liquid bridge experiments use previous literature on a phenomenon named 'liquid bridge', meaning a vertical column of liquid, pinned at each end between planar electrodes, and surrounded by a non-conducting, dielectric gas. These experiments were performed in AC and DC fields; the discussions led to a detailed analysis of this vertical liquid bridge and its stability (Raco 1968; Burcham and Saville 2002; Burcham and Saville 2000; Saville 1997; Gonzalez et al. 1989). These early experiments in vertical jets between charged electrodes also indicate that the longitudinal field along the jet axis has a stabilizing effect on the liquid – gas interface (Melcher and Warren, 1971), which was later also discussed for vertical liquid bridges (Ramos and Castellanos 1993).

In order to discuss horizontal bridges forming in liquids, an experiment first performed by Pellat (1896) was repeated. For this experiment two electrodes are immersed in an insulating, dielectric liquid. The experiment then demonstrates the rise of this fluid between the electrodes when a high-voltage is applied, and is often used to discuss the effects of non-uniform electric fields on liquids (Jones 2002; Melcher 1981). It will be shown that when lifting the electrodes out of the liquid while under voltage, a horizontal bridge forms between the electrodes revealing all the properties previously discussed for a horizontal water bridge.

Experimental setup

For the DC experiments we use two 40 mL glass beakers with spouts, 15 x 5 x 0.25 mm platinum electrodes, a DC high-voltage 0-25 kV power supply Phywe 'Hochspannungs-Netzgerät 25kV' (No 13671.93, Göttingen, Phywe Systeme GmbH, Germany) with a maximum current of 0.5 mA and a 42nF capacitor in parallel to the bridge. For the AC experiments we had a Voltcraft function generator FG 708S (Voltcraft, Germany), a Raveland amplifier XCA 1000 (Raveland, Germany) and a transformer coil with a maximum output of 15 kV at 11.5 kHz. The schematic setup for flow visualisation is shown in Fig. 1.

Alternatively a glass cuvette (Groß-Küvette 700.000, Hellma GmbH & Co. KG, Müllheim Germany) with 50 mm inner width, 50 mm inner height and 10 mm inner depth was used, with or without teflon spacer. This 15 x 10 x 45 mm Teflon

spacer had one rounded side and was glued into a glass cuvette using acrylic glue (Loctite, liquid Cyanacrylat glue, Henkel Central Eastern Europe GmbH, Vienna, Austria).

For imaging a Canon 300D with a Sigma 105mm 1:2.8 macro lens, a Panasonic 3CCD NV-DX100 camcorder with Raynox DCR-150 or Raynox DCR-250 conversion lenses, a Photron FASTCAM SA1 high-speed camera with a Nikkor 60 mm 1:2.8 macro lens, or a CASIO Exilim High Speed EX-F1 - were used. All images were scaled. Infrared imaging (thermal imaging) was done with a FLIR 620 camera (FLIR systems, MA, USA).

While a fluid is electrically stressed, it might be slightly heated (and hence expanded) or compressed. These density changes affect the refractive index and can be recorded within an interferometer. The set-up used is presented in Fig.2 and employed a 20 mW He-Ne laser (NEC cooperation, Japan), several mirrors, beam expanders, beam splitters, lenses and a $\lambda/2$ plate in order to test for polarization effects.

The experiments were performed with a number of polar liquids listed in table 1. For purpose of comparison the non-polar liquid cyclohexane was also tested. All liquids are common solvents and were used in a chemically pure grade. Deionized water was provided by a Barnstead NANOpure type I ultrapure water system (Thermo Fisher Scientific Inc., Waltham, MA) with an initial conductivity of $0.056 \mu\text{S cm}^{-1}$ recorded with the integrated conductivity meter of the system. This conductivity rose quickly to $0.8 \mu\text{S cm}^{-1}$ with a pH value of 5 due to CO_2 saturation under atmospheric conditions (Kendall 1916).

Results and Discussion

Horizontal bridges forming in polar liquids

Do horizontal bridges also form in other fluids than water? The answer is definitely yes. We built horizontal bridges in acetone, dichloromethane (DCM), dimethylformamide (DMF), dimethylsulfoxide (DMSO), ethanol, glycerol (propan-1,2,3-triol), methanol, 1-propanol, 2-propanol, tetrahydrofuran (THF), and water, all polar molecules. Under the experimental conditions presented above we were not able to create a bridge in cyclohexane. As voltage is increased above a threshold value bridge formation usually begins with the ejection of small liquid jets from one or the other beaker, in water accompanied by spark discharges

(Fuchs et al. 2007, Woisetschläger et al. 2010). In methylformamide no bridge is formed under atmospheric conditions, only discharges were observed. Fuchs et al. 2008 tested water bridges in air, nitrogen, oxygen, carbon dioxide and helium atmosphere, with the result that in a helium atmosphere the bridge is replaced by a constant glow discharge between the glass beakers. While in cyclohexane neither fluid motion nor discharge was observed up to 25kV with the beakers in close contact; with methylformamide discharges started at about 3 kV, which is the approximate breakdown voltage in air when the electrode gap is reduced to 3mm. In all other liquids with a relative permittivity larger than 5 and a low-voltage conductivity lower than $0.8 \mu\text{Scm}^{-1}$ jet formation was observed. We would like to point out already in this section that in all polar liquids the conductivity is a function of high-voltage, while Tab.1 gives the low-voltage conductivities.

Horizontal bridges forming in the different fluids are shown in Fig. 3. For THF Fig. 3a shows the maximum length within the voltage range of the power supply. For DMF and water the maximum current of 0.5 mA was reached in Figs.3h and k. The liquids with a low surface tension had a tendency to leak at the spouts (DCM, propanol, acetone, ethanol and methanol).

What holds the bridge against gravity?

To answer this question we varied an old experiment often used to discuss the effects of non-uniform electric fields on liquids – the Pellat experiment (e.g. Jones, 2002). For the set-up we used a glass cuvette with 50 x 50 x 10 mm inner dimensions, the two platinum electrodes, 16 mm apart, and a PVC spacer app. 10 mm thick and 50 mm broad to avoid air breakthrough between the electrodes. For all experiments glycerol (99.9%) was used, with small tracer particles (polyamide spheres, 5 μm diameter) added. Although these tracers can carry charge causing mutual repulsion they give a good impression of the fluid motion.

In 1896 H. Pellat demonstrated the ponderomotive force exerted on a dielectric, non-conductive liquid when two electrodes are dipped into the liquid (Pellat 1896). In Fig. 4 this experiment was repeated. When the voltage between the electrodes was increased the glycerol level rose accordingly (Fig. 4b). At 18 kV DC (approximately the breakdown voltage of air at the distance of the electrode tips), the cuvette was lowered mechanically, leaving a stable, horizontal bridge of glycerol between the electrodes (Figs. 4c and d). Inside the bridge (Figs. 4e and f), polyamide tracer particles indicated a slow motion between the

electrodes, probably caused by cellular convection (Melcher and Taylor 1969). In the outer shell of the bridge a strong rotation existed (Fig.4f), with clockwise rotation direction when looking toward the cathode (in our experiments always at the left side and at ground potential).

The basic principles behind this experiment are well understood and discussed in several textbooks (e.g. Melcher 1981 for the Pellat experiment and Widom et al. 2009 for the horizontal water bridge). The best understanding is through the gradients of the Maxwell pressure, which is part of the Maxwell stress tensor

$$T_{ij} = \epsilon_0 \epsilon_r E_i E_j - \frac{1}{2} \delta_{ij} \epsilon_0 \epsilon_r E_k E_k \quad \text{eq.1}$$

with T_{ij} the stresses in the electric field, E_i the component of the electric field, δ_{ij} the Kronecker delta function, ϵ_0 the vacuum permittivity ($8.85 \cdot 10^{-12} \text{ A s V}^{-1} \text{ m}^{-1}$) and ϵ_r the relative permittivity of the liquid as given in Tab.1. With this approach the pressure in the Bernoulli flow of an adiabatic, incompressible liquid is given by (Widom et al. 2009)

$$p + \frac{1}{2} \rho v^2 + \rho g h - \frac{1}{2} \epsilon_0 (\epsilon_r - 1) E^2 = \text{const} \quad \text{eq. 2}$$

with the pressure p , the fluid density ρ , the fluid velocity v , the height h of the level rise caused by the hydrostatic pressure $\rho g h$, and g the acceleration due to gravity ($g = 9.80665 \text{ ms}^{-2}$). In equilibrium the hydrostatic pressure and the Maxwell pressure counteract, causing a rise of the liquid level as observed in Fig.4b. Using the relation between force density and Maxwell pressure p_{Maxwell}

we obtain the Kelvin force density \vec{f}_{Kelvin}

$$\vec{f}_{\text{Kelvin}} = -\nabla p_{\text{Maxwell}} = \frac{1}{2} \epsilon_0 (\epsilon_r - 1) \nabla (E^2) \quad \text{eq. 3}$$

Thus, the gradient of the Maxwell pressure gives the resulting force on a dielectric liquid in a varying electric field, directing upward into the region of higher field intensity. This relation is valid within a linear dielectric with constant permittivity. Therefore glycerol is pushed into the electric field between the electrodes in Fig.4b because of the force on individual dipoles in the fringing field between the tips of the electrodes.

When discussing the horizontal liquid bridges forming between two beakers as shown in Fig. 3 in terms of the Maxwell pressure, these bridges have a high electric field due to the small cross-section and hence a negative pressure that tends to replenish the liquid within the bridge against drainage.

Especially with long axial lengths horizontal bridges slightly sag under their weight, leading to distortions of the electric field lines inside the bridge. This is schematically plotted in Fig. 5, with the electric displacement field

$\vec{D} \equiv \epsilon_0 \epsilon_r \vec{E}$ as number. Whenever a fluid element wants to drip from the bridge, the concomitant distortion in the electric field will counteract this motion and stabilize the bridge against gravity by the non-zero gradient of the Maxwell pressure (eq.3) and the resulting force density.

Fig. 5 is a numerical simulation of the electric field within the bridge using the electrostatic interface in the AC/DC module in Comsol 4.1 multiphysics software (Comsol Inc., Palo Alto, CA) based on Gauss' law, solving the elements grid with a quadratic interpolation. A 2-dimensional geometry was chosen, with two glass beakers 20mm in width and 10mm height (glass $\epsilon_r = 4.2$), metal electrodes and a water bridge 10mm long with 3mm diameter at the beaker (water $\epsilon_r = 80$), slightly sagging in the middle. Thus, for this simulation of the electric field inside the bridge the surface geometry was that for a stable bridge under equilibrium conditions. The infinite boundary for the mesh was set at a 50 mm radius away from the bridge centre.

With long bridges instabilities can occur, leading to a leaking of the bridge. Such a process is shown for a water bridge at 15 kV DC and 9 mm spout to spout distance in Fig. 6 (two 60 mL beakers, anode beaker right, no capacitor in parallel). A periodic fringe pattern was placed behind the bridge on a glass-ceramic diffuser plate. This fringe pattern is imaged through the water bridge which acts as lens. Assuming a constant refractive index within the bridge, distortions of the otherwise parallel fringe pattern contour its shape.

Without a longitudinal electric field of sufficient strength the leaking water flow decayed into drops by its surface tension (Figs. 6e and f). With a then reduced mass and smaller diameter the leaking of the bridge stopped and the bridge stabilized again. This motion between leakage and no leakage might periodically repeat at low frequency.

When comparing the horizontal bridge between two electrodes in Fig. 4f and the bridge forming between two beakers of glycerol in Fig. 7a, we see a similar flow pattern in both of them. Inside the bridges there is a cellular convection whereas the outer shell rotates. Fig. 7a is an average of 30 exposures, again with tracer particles added. Since polyamide particles can carry charge, it is likely that these tracers are pushed outwards by mutual electrostatic repulsion. Thus in water, tracer particles rotate only at the surface of the bridge (Woisetschläger, 2010) while in glycerol the viscosity is so high that some movement inside the bridge can still be identified.

For liquids with low conductivities, as listed in Tab. 1, Taylor and Melcher developed the leaky dielectric model, reviewed by Melcher and Taylor (1969) and Saville (1997). This model is based on the observation that whenever interfacial regions do exist in a fluid system, and electrical parameters suffer discontinuity, the electromechanics of these interfaces dominate the electrohydrodynamics of the system. If a liquid surface supports a surface charge then tangential electric fields and interfacial electrical shear forces are induced leading to cellular convection in the liquid (Melcher and Taylor, 1969); this can be seen in Fig. 7. It must be mentioned that the bridge itself gives the impression of a cylindrical structure with some rotational symmetry. The electric field outside the bridge certainly does not possess the same geometry because of the non-conducting glass beakers underneath the bridge and the more strongly insulating gas. This asymmetry in the outer field changes the tangential field components around the bridge and must lead to a cellular convection with circumferential components, much more complex than the more or less plane structures presented by Melcher and Taylor (1969).

Finally, with a high voltage of 15 kV AC at 11.5 kHz a glycerol bridge was formed and is shown in Fig. 7a. In the AC field the bridge was smaller and no tracer movement was observed inside the bridge. The DC voltage showed driven flow phenomena associated with the tangential field associated with the surface charge and its relocation, while in the AC field the bridge is closer to the pure dielectric condition, since the AC field tends to suppress effects due to interface charge.

This surface charge and its relocation have an important impact on the bridge morphology. For vertical bridges Saville (1997) showed that within DC

driven bridges leaky dielectrics require lower field strength for stability than perfect dielectrics. This effect will be discussed in the next section.

Stability of the horizontal bridge

By the pressure and viscous stresses, the Maxwell tensor balances the normal and tangential stresses on the bridge liquid/air interface. This tensor was used by Burcham and Saville (2002) to present a theory on the electrohydrodynamic stability on vertical liquid bridges in leaky dielectrics suspended in a dielectric gas. It was this approach which was also used by Widom et al. (2009), Saija et al. (2010) and Marin and Lohse (2010) to discuss horizontal bridges. Additionally, Aerov (2010) pointed at the importance of the surface tension included in the normal stresses at the bridge liquid/air interface.

In order to discuss stability of bridges, Burcham and Saville (2000) defined the following parameters. First the aspect ratio β ,

$$\beta = \frac{l}{d}, \quad \text{eq.4}$$

with l the length and d the diameter of the bridge. Then the ratio of the electric energy contained in the liquid column related to the cylindrical surface energy (electrocapillary number C),

$$C = \frac{\varepsilon \varepsilon_0 E^2 d}{\gamma}, \quad \text{eq.5}$$

with ε the relative permittivity of the liquid (see Tab. 1), ε_0 the vacuum permittivity, E the electric field strength and γ the surface tension of the liquid.

When building bridges in water a relatively small influence of the accurate position of the electrodes in the beakers on the bridge dimensions was observed. This is due to the fact that the relative electric current I through the system with conductivity σ is constant, with the current density j as function of the cross-sectional area A ,

$$I = j A = \sigma E A \quad \text{eq.6}$$

In a first approach the conductivity of water was also assumed to be constant for the tested electric field strengths E inside the water region. From eq. 6 it becomes evident that the electric field strength must be highest in the water bridge section and its closest vicinity (e.g. around the beakers edges). With the

highest resistance and the highest voltage drop in this bridge area, the Ohmic losses must lead to heating, as can be seen in the thermographic image of the water bridge in Fig. 8. The temperature was calculated using an emissivity value of 0.96 for water by a thermal imager (FLIR 620).

A good approach to estimate the electric field strength in the water bridge is shown in Fig. 9. The total DC voltage between the electrodes in the beakers was recorded for constant current $I = 0.5$ mA and different beaker to beaker distances (length). The setup used two 60 mL beakers with 56 mm inner diameter and platinum electrodes in the centres of the beakers. From that line a constant voltage drop of about 5 kV in each beaker was estimated, resulting in a field strength of approximately 6 kV cm^{-1} in bridges between 4 and 16 mm length. The diameter of the bridge changed between 3.0 and 3.7 mm. With this field strength and the observed bridge diameters the electrocapillary number C was between 10 and 13, indicating that the electric energy contained in this geometry was at the same order of magnitude as the energy from surface tension. (A factor of 8 would characterize equal energies, 10 slightly more energy in the electric field.) For better comparison to the data presented by Marin and Lohse (2010) we also used the diameter in eq. 5, while the original papers by Burcham and Saville (2002) write the radius. For the water bridges presented in Fig. 9 the aspect ratios β were between 1 and 5.

Raco (1968) stabilized a vertical liquid bridge between electrodes in air by pulling an electrode out of a pool of liquid, Gonzalez et al. (1989) discussed the stability of such a vertical bridge in a perfect dielectric by solving the electrohydrodynamic equations. Burcham and Saville (2002) did so for vertical bridges formed by leaky dielectrics. They observed that above a certain electric field strength the vertical bridge was a perfect cylinder; when lowering the field strength an amphora-shape, unstable configuration established, with a break-up into separate droplets. These instabilities can also be observed in horizontal bridges as demonstrated in Fig. 10. The recordings in Fig.10 were done with an Exilim EX-F1 high-speed camera at 300 Hz frame rate. In order to get a horizontal bridge at low field strength, a small amount of soap (liquid hand soap) was added to the water used to form a horizontal bridge in two 40 mL beakers. Although the conductivity was increased by the soap, the surface tension

decreased significantly, so that a high voltage below 20kV stabilized bridges with aspect ratios $\beta \geq 20$.

Observed oscillations of such a horizontal water/soap bridge are shown in Fig. 10. Among them is an amphora-shape oscillation, a fundamental, a first harmonic string oscillation and the final break-up with subsequent decay into (charged) droplets. One of the results from the Burcham and Saville (2002) study was that for the stability of a leaky dielectric bridge the electric field parameters are much smaller, due to a larger number of free charges induced at the surface compared to bridges in pure dielectrics. While the normal stresses act to level perturbations, the tangential stresses force the charges on the interface away from bulges in the bridge, so that both effects reduce deformations in leaky dielectric bridges.

Burcham and Saville (2002) also mentioned the effects of the gas / liquid interface on vertical bridges, since conduction in the outer fluid allows charge to leak off the surface, influencing the electric field and the stability of the bridge surface. This effect was observed by us for horizontal bridges (Fig.3) formed in all liquids listed in Tab. 1 by schlieren moving along the bridge surface, indicating distortions in the refractive index. A detailed discussion on these schlieren can be found in Woisetschläger et al. (2010). A possible explanation is the formation of electric double layers along the liquid bridge surface, as found in elektrokinetics and electroosmosis, together with the ionic wind between the electrodes, influencing the surface charges and causing distortions in the electric surface layer. Burcham and Saville (2002) therefore introduced a surface conductivity to explain a different conductivity in the surface layer compared to the bulk. Since this charge transport is anisotropic, distortions in the electric field along the surface might occur, leading to refractive index gradients.

The bridge as electrohydrodynamic pump

During our first investigations of the charge and mass transfer through the bridge we used pH-dye to visualize the flow (Woisetschlaeger et al. 2010). We then showed that the addition of a pH dye does not directly visualize this charge, since it not only raises the conductivity, it also undergoes electrochemical reactions in the electric field (Fuchs et al. 2010a). Therefore a pH dye can be used as tracer for qualitative visualization, but cannot be seen as non-involved indicator since the charges visualized are produced due to its presence. Thus, schlieren and

interferometric techniques are better suited for mass and charge transfer measurements as they are less likely to influence the system under observation.

For that reason the interferometer shown in Fig. 2 detected minute changes in the refractive index while changing the electric field between the electrodes placed in the 50 mm cuvette (compare Fig. 4a and b). The results for glycerol are presented in Fig. 11. Whenever light passes through a refractive index field in a liquid, this wavefront (object beam) suffers a phase lag compared to the wavefront passing through the second, reference beam without liquid. In order to observe a possible refractive index change by the electric force field, an interferogram was recorded without a voltage applied to the electrodes (Fig. 11a) and a second interferogram with 8 kV applied (Fig. 11b). For all recordings one mirror in the interferometer was slightly tilted to superimpose a carrier fringe system which can be modulated by the phase lag caused by the refractive index changes. A fast-Fourier-transformation was then applied to extract the phase information from both interferograms at 0 and 8 kV. Finally, both phase maps were subtracted to obtain the phase change between both exposures without sign ambiguity. In order to calculate the refractive index change from the phase lag, a uniform refractive index distribution over the width of the cuvette (10 mm) was assumed. Finally, three refractive index maps were averaged to reduce the influence of flow instabilities; the resultant map is shown in Fig. 11c. Small scale refractive index distortions along the surface and in the vicinity of the electrodes were also observed, likely caused by distortions of the diffuse electric surface layer. For data reduction software IDEA was used (free download from Graz University of Technology www.optics.tugraz.at; Hipp et al. 2004).

The interferograms were recorded in two sets with the polarization direction either vertical or horizontal. Due to the small Kerr constant of glycerol (Ho and Alfano 1979) no effect of the polarization direction was observed. Thus, the refractive index change recorded is due to a density change, either by pressure or by temperature. Discussing Fig. 11c we can see the consequences of eqs. 1-3. Fluid material was pumped around the sharp edge of the cathode towards higher field strength (increasing refractive index in Fig. 11c). This upward fluid motion lifted the fluid level between the electrodes. But when looking at the anode side, this motion was not symmetrical since along the tip of the anode less fluid was pressed upwards. Such effects were first discussed by Pohl (1958) and Sumoto

(1955) in terms of dielectrophoresis and electrohydrodynamic pumping. Both publications are of high relevance for the horizontal bridge, since Pohl (1958) presented a special electrode configuration which pumped liquid out of a beaker, and both authors observed a different height of liquid rise at anode and cathode for some fluids. Pickard (1962) suggested that “the Sumoto effect appears to be the result of an abnormal fall of potential occasioned by the formation of an ion cloud near one of the electrodes” (Pickard 1962).

In dielectric liquids it is well known that both permittivity and conductivity follow similar trends, they tend to increase or decrease together. This is due to the fact that with an increase in permittivity the electrostatic attraction between ion pairs decreases (Watson 1998). Whenever a high-voltage DC field is applied to the fluid an increasing number of ions escape recombination yielding a change in conductivity, as was discussed by Onsager (1934) and Brière (1964). While at low voltage Ohmic behavior is observed due to ions generated by dissociated molecules, at high voltage the dissociation rate is proportional to the electric field but the recombination rate is not and the current reaches saturation (Jeong and Seyed-Yagoobi 2003; Zhakin 1998). In regions where the dissociation-recombination rate is not in equilibrium complex heterocharge layers build up, inducing a fluid motion in the vicinity of the electrode (Jeong and Seyed-Yagoobi 2004). This fluid motion will lead to friction and cause the change in refractive index close to the electrodes as observed in Fig. 11c. At a certain electric field threshold charge injection from sharp edges might become no longer negligible, the current will increase again (Jeong and Seyed-Yagoobi 2003). All these effects depend also on the electrochemical processes taking place at the electrodes.

This behavior was tested for the geometry used, i.e. the two platinum electrodes were submerged 10 mm deep into the liquid, with 50 mm electrode distance under atmospheric conditions, and electric current and voltage recorded. The result is shown in Fig. 12. The polar liquids used showed non-ohmic behavior indicating that the fluid motion must be also influenced by secondary effects due to heterocharge layers building up close to the electrodes. This behavior causes non-reflection-symmetric boundary conditions for the Maxwell pressure, resulting in a preferred flow direction.

The formation of non-discharged ions at one or both electrodes alter the electric field gradients in the vicinity of the electrodes causing an abnormal fall of

potential and the asymmetry in fluid pressure mentioned previously. To test this effect we used a glass cuvette with a rounded Teflon spacer glued into it (Fig. 13). When a high-voltage was applied to the electrodes the preferred flow direction was towards one electrode and was thus not symmetrical. This effect of asymmetry was also observed in the Pellat experiment and when doing mass flow measurements in the horizontal water bridge (Woisetschläger 2010). When discussing the results in Fig. 13 it became evident that the alcohols used prefer redox reactions with an affinity towards the anode. In other polar fluids the cathode electro-chemical reactions have a higher level than the anode one (Zhakin 1998). Therefore non-equilibrium heterocharge layers in some alcohols will build up faster at the anode than at the cathode, causing a difference in Maxwell pressure between the two electrodes (Fig. 13 left side), counteracted only by the hydrostatic pressure and the rim of the beaker. Electrochemical reactions of organic solvents in a horizontal bridge set-up have been described in detail for phenol and glycol solutions (Eisenhut et al. 2011).

In the vicinity of the electrodes a strong fluid motion parallel to the surface was observed. This is essentially how electrowetting works – when the Maxwell pressure drives contact-line motion (Jones 2002).

Compared to other polar liquids, in water nearly no or only little preferred flow direction through the bridge was observed (Woisetschläger 2010), enabling the bridge to stabilize for hours when platinum electrodes are used, preventing metal ions to dissolve. This stabilization is possible since long term thermographic visualizations suggest a permanent directional change of flow direction through the bridge in the 5-20 Hz range. Similar effects were observed with other low-viscosity liquids, as methanol.

Conclusion

A ‘floating water bridge’ forms when glass beakers are filled with deionised water and a DC voltage between 10 kV and 20 kV is applied under atmospheric conditions. By repeating a version of Pellat’s experiment it was experimentally proven that such horizontal bridges can be explained by electrohydrodynamic relations only. They are stable by the action of electrohydrodynamic pressure, and furthermore, all static and dynamic properties of the phenomenon called a ‘floating water bridge’ can be discussed by the gradient of

Maxwell pressure, replenishing the liquid within the bridge against any drainage mechanism. In a large number of other polar liquids tested, and having a relative permittivity larger than 5 and a not too high conductivity under the influence of an electric field (as in methylformamide), a horizontal bridge did form as well. On the one side a persistent pumping of the liquid from one beaker into the other was observed due to the gradients in Maxwell pressure. On the other side non-equilibrium heterocharge layers accumulate at the electrodes, presumably driven by electrochemical reactions, cause non-uniformities in the Maxwell pressure driven fluid motion and therefore result in a preferred flow direction through the bridge. These non-uniformities in mass flow through the horizontal bridges were also discussed by a second experiment in a single beaker configuration.

Since polar liquids represent leaky dielectrics, the liquid surfaces conduct surface charges, interfacial electrical shear forces will be induced, leading to cellular convection in the bridge, together with reported instabilities of the system. Under the conditions discussed - electrocapillary number C between 10 and 13 and field strengths of $5-7 \text{ kV cm}^{-1}$ - horizontal bridges of polar liquids can be operated under atmospheric conditions and provide a laboratory of their own.

Outlook

The experiments presented demonstrate that a horizontal liquid bridge provides interesting new possibilities to study basic interactions between electric fields and fluids, and introduces a novel environment for (electro-)chemical reactions: Substances which remain mostly inert in the process could be brought in contact with other educts to chemically react within the bridge; substances which do react electrochemically might do this in a different manner, which could be used to specifically select one chemical pathway over others, or stop an oxidation process at an – otherwise possibly short-lived – intermediate (Eisenhut et al. 2011). By applying different potentials the electrochemical environment can be changed without the addition of an acid or base; at the same time educts could be oxidized to a more reactive form. This could be used e.g. to start polymerization reactions of ultra-pure monomers in bridge building solvents like methanol. The affinity of certain liquids to one electrode can be used to separate them in the process. These possibilities should be considered exemplary for a large number of possible industrial applications of the techniques presented.

Finally, from a microbiological point of view, liquid bridge mechanisms could be important to further understand charge and substance transport through the cell membrane. Since the potential differences there are of comparable magnitude or even larger (e.g. Hülshager 1983), we suggest that microscopic bidirectional electrohydrodynamic flows may play a role within or next to the established mechanisms.

Acknowledgements

This work was performed in the TTIW-cooperation framework of Wetsus, Centre of Excellence for Sustainable Water Technology (www.wetusus.nl) together with Graz University of Technology, Austria (www.tugraz.at). Wetsus is funded by the Dutch Ministry of Economic Affairs, the European Union Regional Development Fund, the Province of Fryslân, the City of Leeuwarden, the EZ/Kompas program of the "Samenwerkingsverband Noord-Nederland" and the participating companies. The authors would like to thank the whole research team and staff of WETSUS, the Institute of Analytical Chemistry and Food Chemistry at the Graz University of Technology, especially Dr. Xinghua Guo for providing some of the solvents, and the Institute of Hydraulic Engineering and Water Resources at Graz University of Technology for sharing the Photron high speed camera. With great pleasure, the authors furthermore wish to thank Profs. Marie-Claire Bellissent-Funel (Laboratoire Léon Brillouin, Saclay), Eshel Ben-Jacob (Tel Aviv University), Mariano Bizzarri (Università La Sapienza, Roma), Harry Bruning (Wetsus), Cees Buisman (Wetsus), Gert-Jan Euverink (Wetsus), Friedemann Freund (NASA SETI Institute, California), Emilio Del Giudice (Università di Milano), Ferenc Hajdu (Central Research Institute for Chemistry, Hungarian Academy of Sciences, Budapest), Franz Heitmeir (Graz University of Technology), Hideo Nishiumi (Chem. Eng. Lab., Hosei University, Japan), Laurence Noirez (Laboratoire Léon Brillouin, Saclay), Gerald H. Pollack (University of Washington), Alan Soper (Rutherford Appleton Laboratories, ISIS, Oxford), Piergiorgio Spaggiari (Istituti Ospitalieri Di Cremona, Milano, Italy), José Teixeira (Laboratoire Léon Brillouin, Saclay), Giuseppe Vitiello (Università degli studi di Salerno), Vladimir Voeikov (M.V. Lomonosov Moscow State University), John Watterson (Ashmore, Australia) as well as Luewton L.F. Agostinho, Cees Kamp, Astrid H. Paulitsch-Fuchs, Martina Sammer and Doekle Yntema (Wetsus) for the ongoing discussion on the water bridge phenomenon (in alphabetic order).

References

- Aerov AA (2010) Why the Water Bridge does not collapse, *Phys. Rev. E* 84 (2011) 036314
- Armstrong, Lord W. (1893) Electrical Phenomena. *The Electrical Engineer* 1893, 10 February, 154-155.
- Briere GB (1964) Electrical conduction in purified polar liquids, *British Journal of Applied Physics* 15 (4), art. no. 310, pp. 413-417
- Burcham CL, Saville DA (2000) Electrohydrodynamic stability of a liquid bridge: Microgravity experiments on a liquid bridge suspended in a dielectric gas, *J. Fluid Mech.* 405, 37-56.
- Burcham CL, Saville DA (2002) Electrohydrodynamic stability: Taylor-Melcher theory for a liquid bridge suspended in a dielectric gas, *J. Fluid Mech.* 452, 163-187
- Del Giudice E, Fuchs EC, Vitiello G (2010) Collective Molecular Dynamics of a Floating Water Bridge, *WATER (Seattle)* 2, 30 July 2010, 69-82
- Eisenhut M, Guo, X, Paulitsch-Fuchs, AH, Fuchs, EC (2011) Aqueous phenol and ethylene glycol solutions in electrohydrodynamic liquid bridging, *Cent. Eur. J. Chem.* 9(3), 391-403
- Fuchs EC (2010) Can a Century Old Experiment Reveal Hidden Properties of Water?, *Water (MDPI)* 2010, 2, 381-410
- Fuchs EC, Woisetschläger J.; Gatterer, K.; Maier, E.; Pecnik, R.; Holler G, Eisenkölbl H (2007) The floating water bridge. *J. Phys.-D-Appl. Phys.* 2007, 40, 6112-6114.
- Fuchs EC, Gatterer, K.; Holler, G.; Woisetschläger, (2008) Dynamics of the floating water bridge, *J. Phys.-D-Appl. Phys.*, 41, 185502-185507
- Fuchs EC, Bitschnau, B.; Woisetschläger, J.; Maier, E.; Beuneu B.; Teixeira, J. (2009) Neutron Scattering of a Floating Heavy Water Bridge. *J. Phys.-D-Appl. Phys.*, 42, 065502:1-065502:4.
- Fuchs EC, Agostinho LLF, Eisenhut M, Woisetschläger J, (2010a) Mass and charge transfer within a floating water bridge, *Laser Applications in Life Sciences, Proc.SPIE, Vol.7376, 73761E1-15*
- Fuchs EC, Baroni, P.; Bitschnau, B.; Noirez, L. (2010b) Two-Dimensional Neutron Scattering in a Floating Heavy Water Bridge. *J. Phys.-D-Appl. Phys.*, 43, 105502:1-105502:5.
- Fuchs EC, Agostinho LLF, Wexler A, Wagterveld RM, Tuinstra J, Woisetschläger J (2011a) The behaviour of a floating water bridge under reduced gravity conditions, *Journal of Physics D: Appl. Phys.*, 44, 025501
- Fuchs EC, Bitschnau B, Di Fonzo S, Gessini A Woisetschläger J, and Bencivenga F (2011b), Inelastic UV scattering in a floating waterbridge, *J. Phys. Sc. Appl.* 1 No. 3, 2011 (in press)
- Gonzalez H, McCluskey FMJ, Castellanos A, Barrero A (1989) Stabilization of dielectric liquid bridges by electric fields in the absence of gravity, *J. Fluid Mech.* 206, 545 (1989).
- Hipp M, Woisetschläger J, Reiterer P, Neger T (2004) Digital evaluation of interferograms, *Measurement, Elsevier, Vol.36, pp53-66*
- Ho PP, Alfano RR (1979) Optical Kerr effect in liquids, *Phys. Rev. A* 20, 2170–2187

- Hülshager H, Potel J, Niemann EG, Electric Field Effects on Bacteria and Yeast Cells, *Radiat. Environ. Biophys.* 22, 149-162 (1983)
- Jeong SI, Seyed-Yagoobi J (2003) Theoretical/Numerical Study of Electrohydrodynamic Pumping Through Conduction Phenomenon, *IEEE Transactions on Industry Applications*, 39, 355-361
- Jeong SI, Seyed-Yagoobi J (2004) Fluid Circulation in an Enclosure Generated by Electrohydrodynamic Conduction Phenomenon, *IEEE Transactions on Dielectrics and Electrical Insulation*, 11, 899-910
- Jones TB (2002) On the relationship of dielectrophoresis and electrowetting, *Langmuir* 18, 4437-4443
- Kendall J (1916) The specific conductivity of pure water in equilibrium with atmospheric carbon dioxide. *J Am Chem Soc* 38, 1480–1497
- Marin AG, Lohse D (2010) Building water bridges in air; Electrohydrodynamics of the floating water bridge, *Physics of Fluids* 22, 122104.
- Melcher JR (1981) *Continuum Electromechanics*. Cambridge, MA: MIT Press, 1981. Copyright Massachusetts Institute of Technology. ISBN: 9780262131650. Also available online from MIT OpenCourseWare at <http://ocw.mit.edu> (accessed 01 19, 2011) under Creative Commons license Attribution-NonCommercial-Share Alike.
- Melcher JR and Taylor GI (1969) Electrohydrodynamics: A Review of the role of interfacial shear stresses, *Annu. Rev. Fluid Mech.* 1969.1:111-146
- Melcher JR and Warren EP (1971) Electrohydrodynamics of a current carrying semi-insulating jet, *J. Fluid Mech.* 47, 127 – 143, 2 plates
- Nishiumi H, Honda F (2009) Effects of Electrolyte on Floating Water Bridge, *Res. Lett. Phys. Chem.* 2009, 371650 (3pp).
- Onsager L (1934) Deviations from Ohm's law in weak electrolytes, *The Journal of Chemical Physics* 2 (9), pp. 599-615
- Pellat H 1896 Mesure de la force agissant sur les diélectriques liquides non électrisés placés dans un champ élitrique. *C. R. Acad. Sci. Paris* 123, 691-696.
- Pickard WF (1962) An Explanation of the de Sumo to Effect, *Journal of Applied Physics*, 33, 941-942
- Pohl HA (1958) Some effects of nonuniform fields on dielectrics, *Journal of Applied Physics* 29 (8), pp. 1182-1188
- Ponterio, R.C.; Pochylski, M.; Aliotta, F.; Vasi, C.; Fontanella, M. E.; Saija, F. (2010) Raman scattering measurements on a floating water bridge. *J. Phys.-D-Appl. Phys.*, 43, 175405:1-175405:8.
- Raco RJ (1968) Electrically supported column of liquid, *Science*, Vol. 160, Issue 3825, 311-312
- Ramos A, Castellanos A (1993) Bifurcation diagrams of axisymmetric liquid bridges of arbitrary volume in electric and gravitational axial fields, *Phys. Fluids* 6, 207 – 225
- Riddick JA, Bunger WB (1989) *Organic solvents: Physical properties and methods of purification*, Wiley, ISBN 978-0471-08467-9

- F. Saija, Aliotta F, Fontanella ME, Pochylski M, Salvato G, Vasi C, Ponterio RC (2010)
Communication : An extended model of liquid bridging, *J. Chem. Phys.* 133, 081104
- Saville DA (1997) Electrohydrodynamics: The Taylor-Melcher Leaky dielectric model, *Ann. Rev. Fluid Mech.*, 29, 27-64
- Sumoto I (1955) An interesting phenomenon observed on some dielectrics, *Journal of the Physical Society of Japan* 10 (6), pp. 494
- Watson PK (1998) Conduction, instabilities and breakdown in liquid dielectrics, in: Castellanos A (ed) (1998) *Electrohydrodynamics*, International Centre for Mechanical Sciences, CISM Courses and Lectures No. 380, Springer, Wien, ISBN 3-211-83137-1
- Widom, A.; Swain, J.; Silverberg, J.; Sivasubramanian, S.; Srivastava, Y.N. (2009) Theory of the Maxwell pressure tensor and the tension in a water bridge. *Phys. Rev. E* 2009, 80, 016301:1-016301:7.
- Wohlfarth CH ed. (2008) *SpringerMaterials - The Landolt-Börnstein Database* (<http://www.springermaterials.com>). Springer-Verlag Berlin Heidelberg, DOI: 10.1007/978-3-540-75508-1_31
- Woiseschläger, J.; Gatterer, K.; Fuchs, E.C. (2010) Experiments in a floating water bridge. *Exp. Fluids*, 48-1, 121-131
- Zhakin AJ (1998) Conduction phenomena in dielectric liquids, in: Castellanos A (ed) (1998) *Electrohydrodynamics*, International Centre for Mechanical Sciences, CISM Courses and Lectures No. 380, Springer, Wien, ISBN 3-211-83137-1

Figures with captions

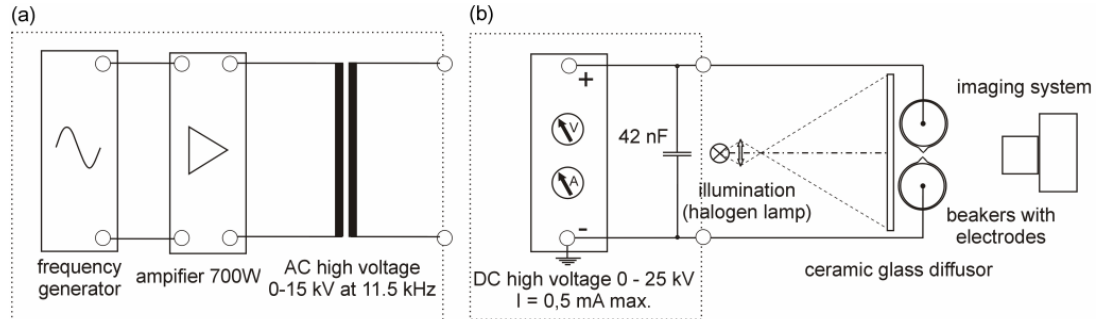


Fig.1 Experimental set-up for the visualization of horizontal bridges between two beakers. (a) AC setup including frequency generator, amplifier and transformer coil, (b) DC setup including power supply, illumination, ceramic glass diffuser, beakers and imaging system.

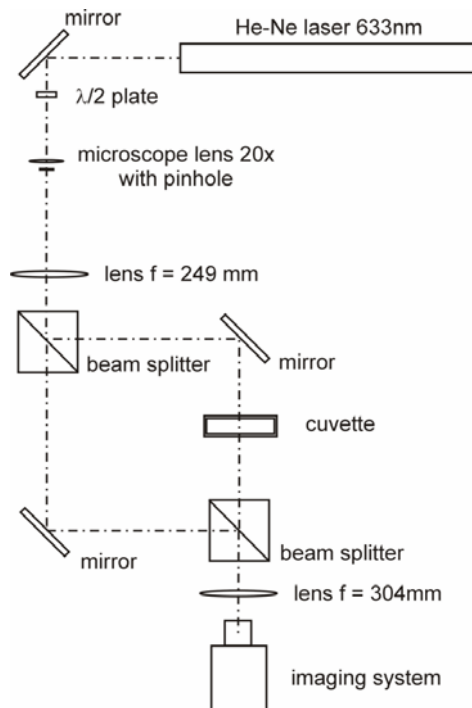


Fig.2 Mach-Zehnder type interferometer used to record the changes in refractive index when a high voltage was applied to the liquid in the cuvette. The base length of the interferometer was 300x300mm, the beam splitter cubes had 50mm cubic side length.

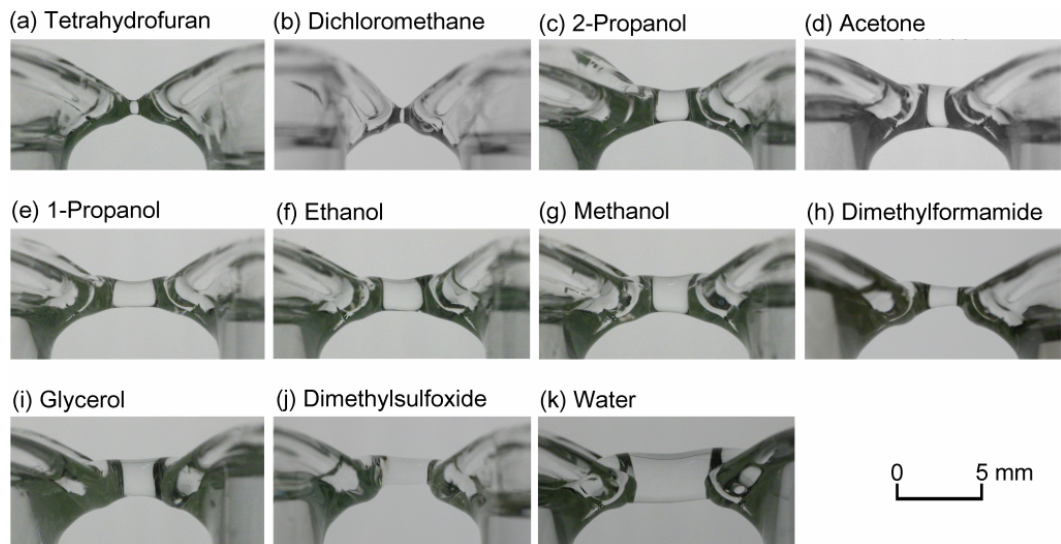


Fig.3 horizontal bridges forming in different polar liquids under atmospheric conditions and DC voltage. (a) Tetrahydrofuran 16 kV, (b) dichloromethane 19 kV, (c) 2-propanol 8 kV, (d) acetone 10 kV, (e) 1-propanol 10 kV, (f) ethanol 9.5 kV, (g) methanol 9.5 kV, (h) dimethylformamide 12.5 kV, (i) glycerol 11.5 kV, (j) dimethylsulfoxide 12 kV , (k) water 12 kV.

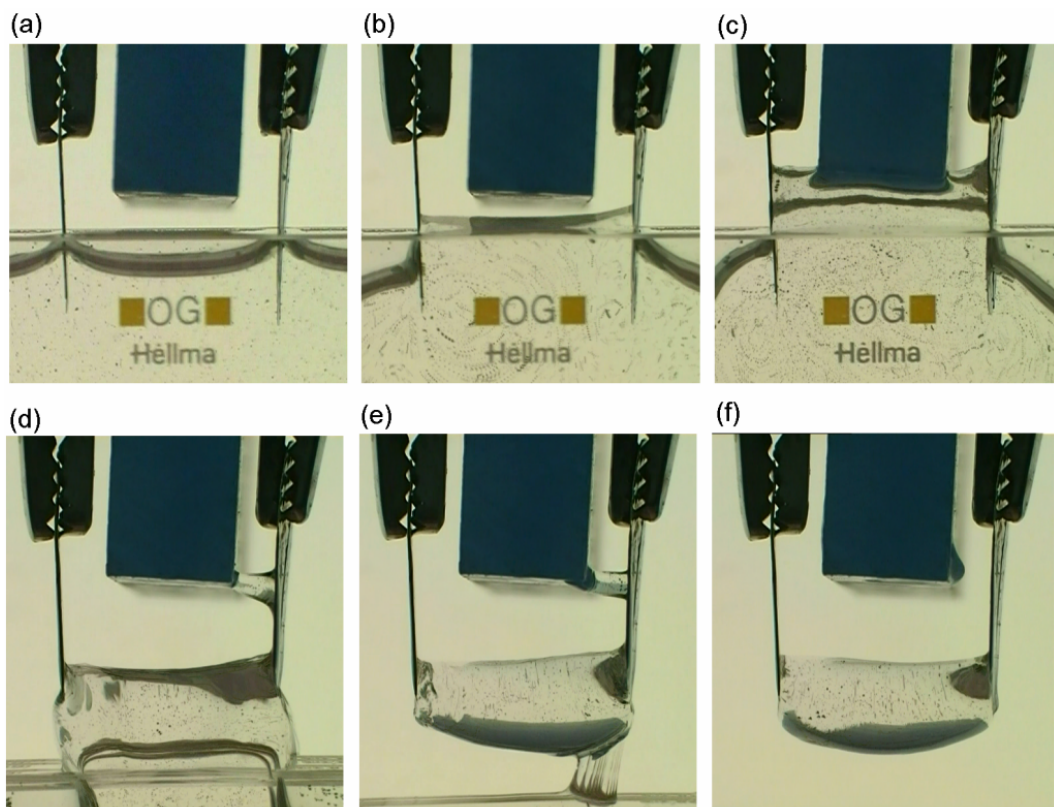


Fig.4 Pellet experiment to form a horizontal bridge in glycerol pinned between two electrodes. (a) set-up 0kV, (b) 13kV DC, (c) to (f) 18kV DC. The glass cuvette was lowered mechanically between (c) and (f). (b) to (f) are averages of 6 images to better visualize the tracer particle motion.

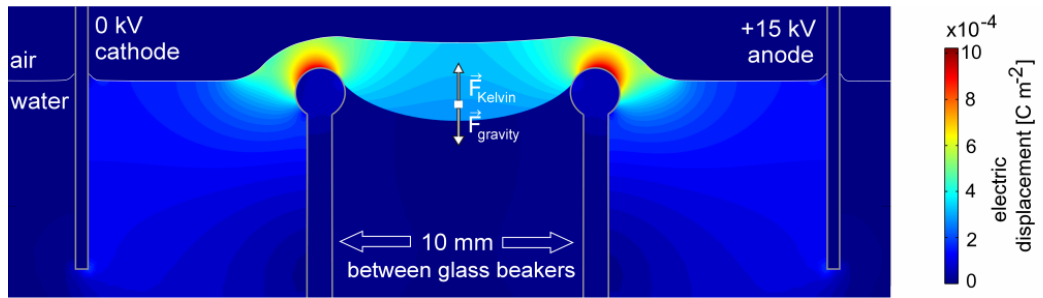


Fig.5 Numerical simulation of the electric field within the water bridge using Comsol 4.1 software. Displayed are the absolute values of the electric displacement field. Ground potential is at infinity, cathode is at 0 kV (left), anode at 15 kV (right). The glass beakers have a slightly rounded brim. The Kelvin force density counteracts gravitational force.

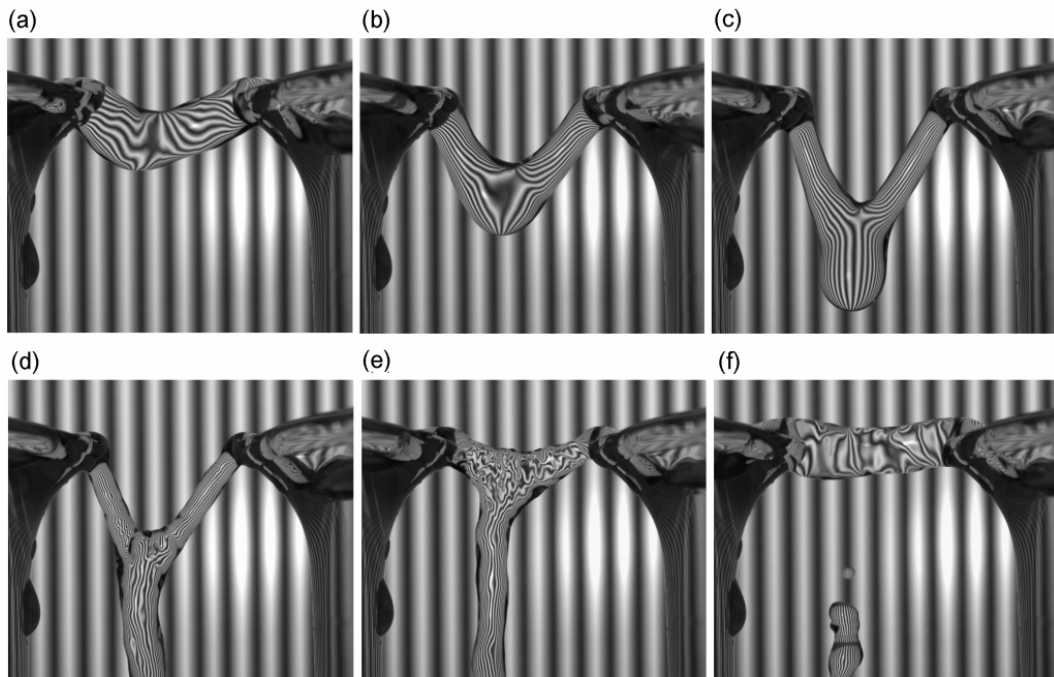


Fig.6 Especially with long bridges instabilities can occur leading to a leaking of the bridge. These high-speed images were recorded at 0.25 seconds intervals with a periodic fringe pattern placed behind the bridge contouring its shape. Distortions of the otherwise parallel fringe pattern contour the shape of the bridge.



Fig.7 (a) Horizontal liquid bridge in glycerol formed between two beakers, 16 kV DC. Polyamide tracers were added for stream line visualization, the picture is a 30 frames average. (b) Horizontal bridge formed at 15 kV AC, 11.5 kHz. No tracer movement can be observed.

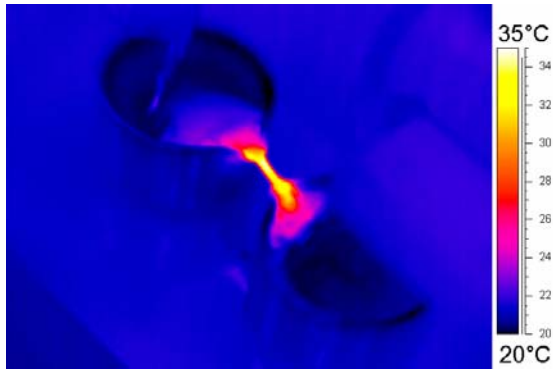


Fig.8 Thermographic image of a water bridge (12 kV DC, 9 mm beaker to beaker distance).

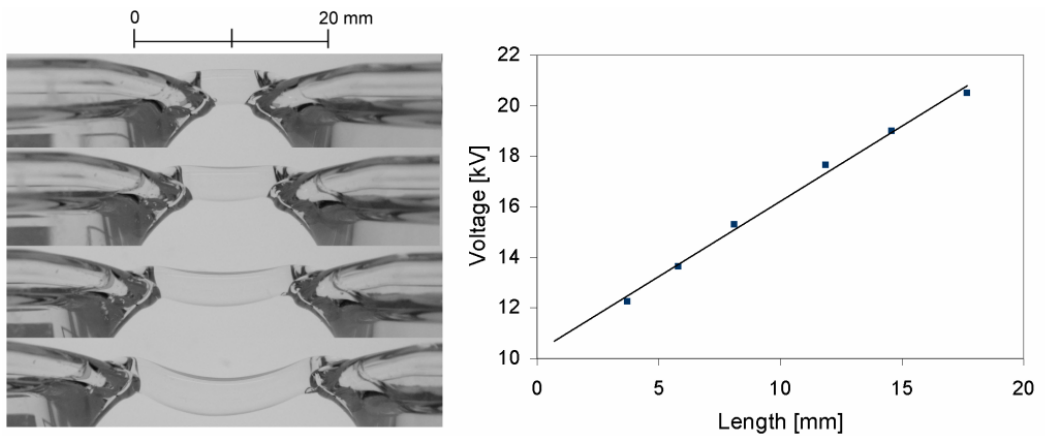


Fig.9 DC voltage applied to the electrodes in the beaker vs. the spout to spout distance (length of the bridge) for a water bridge. Current was constant at 0.5 mA.

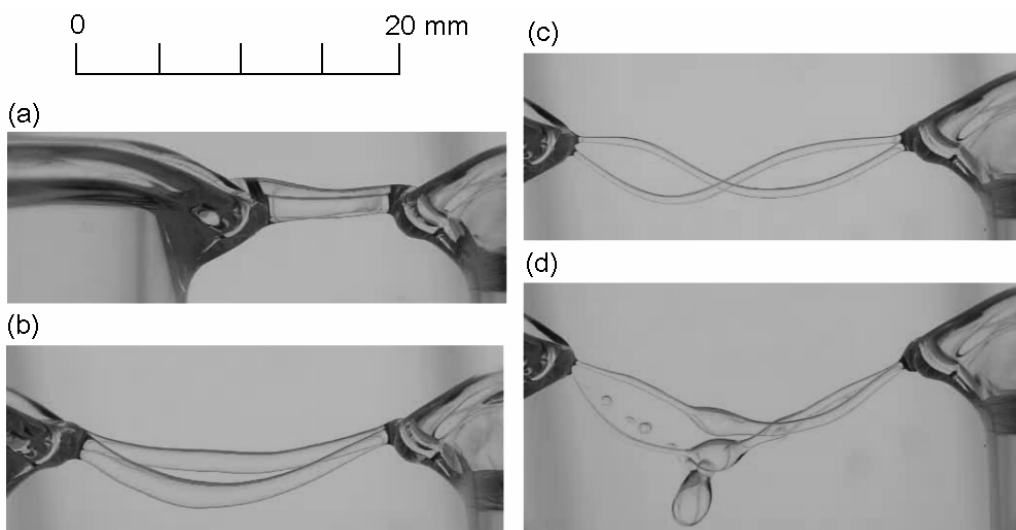


Fig.10 Oscillations of a water bridge with a small amount of soap added. (a) 13 kV, (b-d) 17 kV applied to the electrodes. (a) shows a amphora type oscillation (1/10 s interval), (b) fundamental string oscillation (1/15 s interval), (c) first harmonic (1/30 s interval) and (d) bridge break-up (1/75 s interval). All images are multiple exposures.

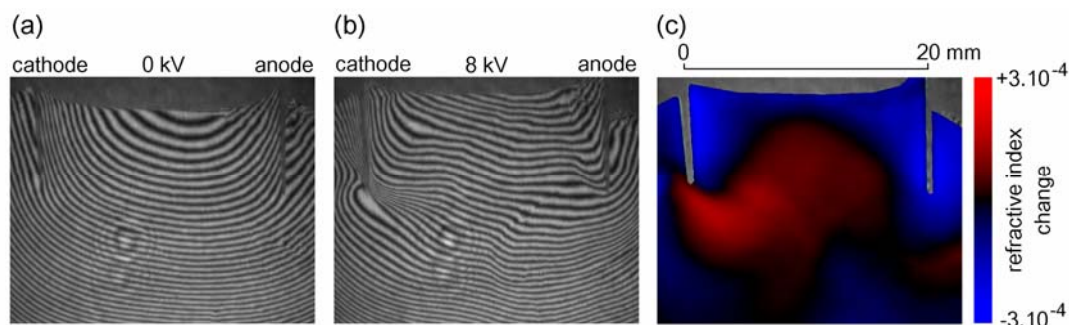


Fig.11 Interferograms reveal changes in the refractive index due to the application of a high-voltage DC field in glycerol. (a) reference recording at 0 kV, (b) high-voltage interferogram, (c) change in refractive index calculated from the phase shifts recorded in (a) and (b).

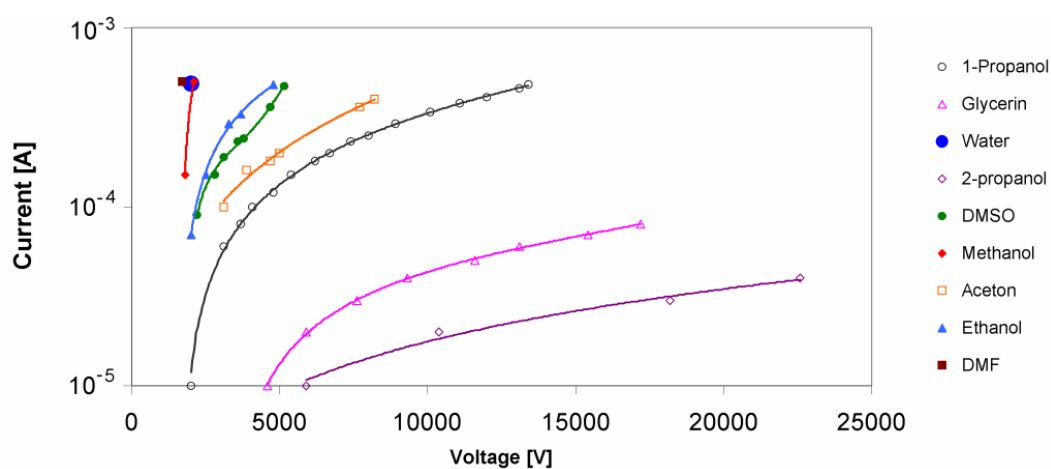


Fig.12 Non-ohmic behaviour of the polar liquids used to form a horizontal bridge. The recordings were done up to 25 kV and up to 0.5 mA. The platinum electrodes dipped 10 mm deep into the liquid with 50 mm electrode distance under atmospheric conditions.

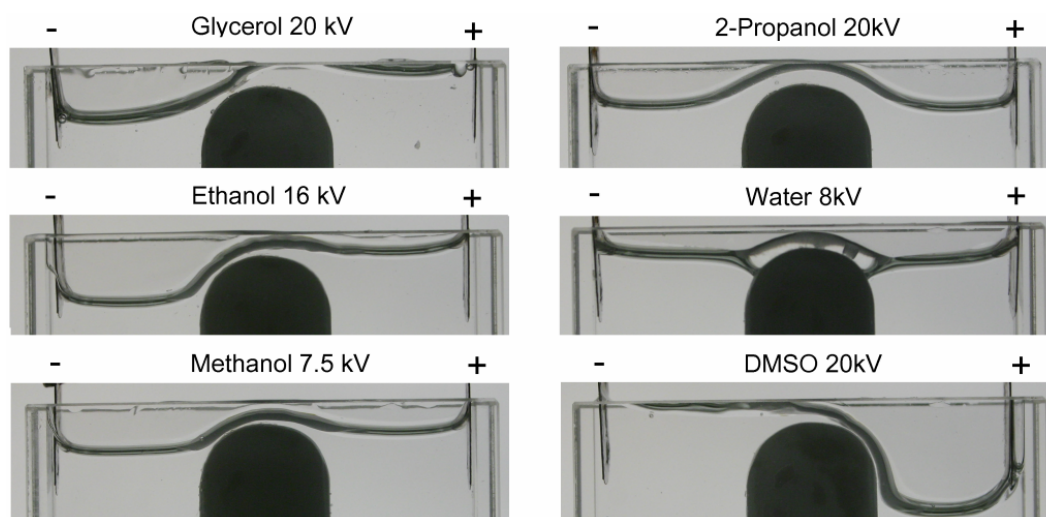


Fig.13 Electrohydrodynamic pumping of polar liquids under the influence of a high-voltage DC field through a horizontal bottle neck (experimentally simulated “bridge”).

Table with caption

Table. 1 Liquids tested in a horizontal bridge (data at 298 K from Riddick and Bunger 1986; Wohlfarth 2008).

Name	relative permittivity (static)	Conductivity [$\mu\text{S cm}^{-1}$]	Dynamic viscosity [mPa s]	surface tension [mN m^{-1}]	density [kg m^{-3}]
Cyclohexane	2.02	0.05	0.883	24.4	773.9
Tetrahydrofuran	7.36	0.048	0.471	27.04	881.9
Dichloromethane	8.51	0.000043	0.413	27.2	1316.6
2-Propanol	19.45	0.058	2.039	21.1	780.7
Acetone	20.59	0.005	0.303	22.7	784.3
1-Propanol	20.73	0.00917	1.952	23.1	798.9
Ethanol	24.35	0.00135	1.067	22.3	784.9
Methanol	33.77	0.0015	0.542	22.1	768.3
Dimethylformamide	37.65	0.06	0.796	36.3	943.8
Glycerol	42.49	0.06	987.8	63.0	1258.1
Dimethylsulfoxide	47.13	0.002	1.98	42.8	1095.4
Water, deionised	79.5	0.05	0.89	72.01	997.1
Methylformamide	176.54	0.8	1.65	39.58	966.6